ISSN 1070-3284, Russian Journal of Coordination Chemistry, 2015, Vol. 41, No. 6, pp. 353–361. © Pleiades Publishing, Ltd., 2015.
Original Russian Text © R.A. Polunin, V.N. Dorofeeva, A.E. Baranchikov, V.K. Ivanov, K.S. Gavrilenko, M.A. Kiskin, I.L. Eremenko, V.M. Novotortsev, S.V. Kolotilov, 2015, published in Koordinatsionnaya Khimiya, 2015, Vol. 41, No. 6, pp. 323–331.

Influence of Morphology and Defects in Crystals of Porous Coordination Polymers on the Sorption Characteristics

R. A. Polunin[a], V. N. Dorofeeva[a], A. E. Baranchikov[b], V. K. Ivanov[b], K. S. Gavrilenko[c], M. A. Kiskin[b, *], I. L. Eremenko[b], V. M. Novotortsev[b], and S. V. Kolotilov[a]

[a] *Pisarzhevskii Institute of Physical Chemistry, National Academy of Sciences of Ukraine, Kiev, Ukraine*

[b] *Kurnakov Institute of General and Inorganic Chemistry, Russian Academy of Sciences, Leninskii pr. 31, Moscow, 119991 Russia*

[c] *Scientific Educational Chemical Biological Center, Shevchenko National University, Kiev, Ukraine*

**e-mail: mkiskin@igic.ras.ru*

Received December 1, 2014

Abstract—Porous coordination polymers $[Fe_2MO(Piv)_6(L)_x]_n$ (L is tris(4-pyridyl)pyridine, M = Ni (**I**) and Co (**II**); L is tris(4-pyridyl)triazine, M = Ni (**III**) and Co (**IV**); x varies from 0.7 to 1.17) are obtained. The structure of polymer **I** is determined by X-ray diffraction analysis. The choice of the solvent (chloroform or dimethylformamide (DMF)) for the preparation of polycrystalline samples affects the morphology of the crystals. It is found for the studied samples that an increase in the average crystal size (from 1 to 20 μm) and the enhancement of the crystallinity of the samples increase the sorption capacity with respect to hydrogen from 0.7 to 0.9% (78 K, 1 atm).

DOI: 10.1134/S1070328415060056

INTRODUCTION

Porous coordination polymers are promising for the development of materials that can be used for the storage and selective sorption or separation of gases, as well as catalysts, active cells of sensors, etc. [1, 2]. A series of works published presently shows the influence of the structure of porous coordination polymers (in particular, the bridging ligand size) and chemical nature of metal-containing units or organic ligands on the sorption characteristics of these compounds [3, 4]. However, in spite of the influence of the synthesis conditions on the morphology of the porous coordination polymers and, as a consequence, on their sorption properties [5], a relationship between these characteristics remains poorly studied.

The aim of this work is to determine the influence of the crystal size and morphology and the level of crystallinity of the samples (which can be characterized by the reflection half-width in the diffraction pattern) on the sorption characteristics of the porous coordination polymer $[Fe_2NiO(Piv)_6(L)_x]_n$ (L is 2,4,6-tris(4-pyridyl)pyridine (L^1) or 2,4,6-tris(4-pyridyl)triazine (L^2), and x varies from 0.7 to 1.17, depending on the preparation conditions of the porous coordination polymers).

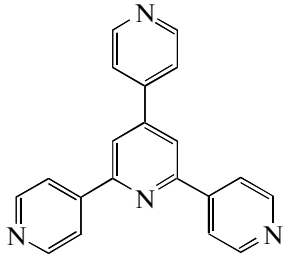

(L^1)

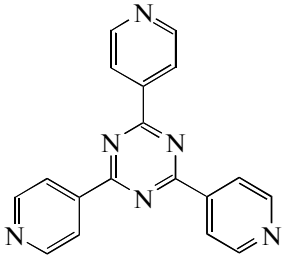

(L^2)

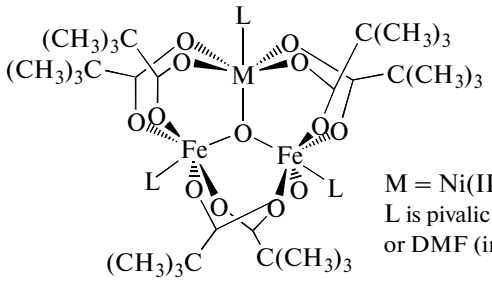

M = Ni(II) or Co(II)
L is pivalic acid
or DMF (in solution).

We have previously described a series of porous coordination polymers of the composition $[Fe_2MO(Piv)_6(L)_x]_n$ (L is a ligand of the bipyridine or tripyridine series; $x = 1.5$ or 1, respectively) [6–8]. Among these compounds, complex $[Fe_2MO(Piv)_6(L^1)]_n$ is characterized by the highest Brunauer–Emmett–Teller (BET) surface area S_{BET} = 730 m^2/g and a pore volume of 0.28 cm^3/g (the porous coordination polymer sorbs 0.91% H_2 at 1 atm and 78 K) [6]. In addition to the high sorption characteristics, the crystal lattice of this porous coordination polymer is conformationally rigid and the pore size and sorption characteristics of the complex are independent of the substrate nature (unlike the porous coordination polymers with conformationally labile crystal lattices [7, 8]). For these reasons, the porous coordination polymer $[Fe_2MO(Piv)_6(L^1)]_n$ and the isostructural complex containing an electron-deficient analog of L^1, 2,4,6-tris(4-pyridyl)triazine (L^2), were chosen for the study of the influence of the synthesis conditions on the morphology and particle size.

In this work, we prepared porous coordination polymers $[Fe_2MO(Piv)_6(L)_x]_n$, where M = Ni and Co; L = L^1 (**I** and **II**, respectively) or L^2 (**III** and **IV**, respectively). The samples obtained from chloroform are designated as $\mathbf{I}^C$–$\mathbf{IV}^C$, and those obtained from DMF are designated as $\mathbf{I}^D$–$\mathbf{IV}^D$. The samples were characterized by scanning electron microscopy (SEM) and X-ray powder diffraction (XPRD) analysis, and their sorption properties were studied. The structure of compound **I** was characterized by single-crystal X-ray diffraction analysis.

EXPERIMENTAL

All procedures related to the synthesis of new complexes were carried out in air using commercial solvents and reagents (DMF, chloroform, dioxane, and ethanol). The starting trinuclear complexes $[Fe_2MO(Piv)_6(HPiv)_3]$ (M = Ni and Co) and ligands L^1 and L^2 were synthesized using known procedures [8–10].

General synthesis of $[Fe_2MO(Piv)_6(L)_x]_n$ (L = L^1 and L^2) in chloroform. Equivalent amounts of $Fe_2NiO(Piv)_6(HPiv)_3$ and ligand L (molar ratio 1 : 1) taken separately were dissolved in a minimum volume of chloroform at 50°C. The obtained saturated solutions were filtered from a minor amount of undissolved admixtures on a paper filter, after which a hot solution of the ligand was poured through a paper filter to the preliminarily filtered hot solution of $Fe_2NiO(Piv)_6(HPiv)_3$. The immediate formation of a finely crystalline precipitate of the complex was observed. The precipitate was filtered off on a glass filter and washed with boiling chloroform (40 cm^3). The yield was ~50–60%.

$[Fe_2NiO(Piv)_6(L^1) \cdot 0.43Fe_2NiO(Piv)_6 \cdot 2.5HPiv \cdot 2.5H_2O \cdot 0.67CHCl_3]_n$ ($\mathbf{I}^C \cdot 2.5HPiv \cdot 2.5H_2O \cdot 0.67CHCl_3$; $x = 0.7$).

For $C_{72.46}H_{115.39}N_4Cl_2O_{24.64}Fe_{2.86}Ni_{1.43}$

anal. calcd., %:	C, 49.70;	H, 6.64;	N, 3.20.
Found, %:	C, 49.68;	H, 6.61;	N, 3.19.

$[Fe_2CoO(Piv)_6(L^1) \cdot 0.18Fe_2CoO(Piv)_6 \cdot HPiv \cdot 0.85H_2O \cdot 2.55CHCl_3]_n$ ($\mathbf{II}^C \cdot HPiv \cdot 0.85H_2O \cdot 2.55CHCl_3$; $x = 0.85$).

For $C_{63.29}H_{92.22}N_4O_{18.14}Cl_9Fe_{2.36}Co_{1.18}$

anal. calcd., %:	C, 44.20;	H, 5.40;	N, 3.25.
Found, %:	C, 44.29;	H, 5.42;	N, 3.26.

$[Fe_2NiO(Piv)_6(L^2) \cdot 0.075L^2 \cdot 1.45H_2O]_n$ ($\mathbf{III}^C \cdot 1.45H_2O$; $x = 1.075$).

For $C_{49.35}H_{69.8}N_{6.45}O_{14.45}Fe_2Ni$

anal. calcd., %:	C, 51.33;	H, 6.09;	N, 7.82.
Found, %:	C, 51.32;	H, 6.09;	N, 7.82.

$[Fe_2CoO(Piv)_6(L^2) \cdot 0.17L^2 \cdot 0.15HPiv \cdot 0.7H_2O]$ ($\mathbf{IV}^C \cdot 0.15HPiv \cdot 0.7H_2O$; $x = 1.17$).

For $C_{51.81}H_{70.94}N_{7.02}O_{14}Fe_2Co$

anal. calcd., %:	C, 52.46;	H, 6.02;	N, 8.29.
Found, %:	C, 52.38;	H, 6.01;	N, 8.30.

General synthesis of $[Fe_2MO(Piv)_6(L)_x]_n$ (L = L^1 and L^2) in DMF. Equivalent amounts of $Fe_2NiO(Piv)_6(HPiv)_3$ and ligand L (molar ratio 1 : 1) were dissolved separately in a minimum amount of DMF at 140–155°C. An excess of pivalic acid (molar ratio 1 : 5) was added to a solution of the ligand. The obtained solutions were filtered from a minor amount of undissolved admixtures on a paper filter, after which a hot solution of the ligand with pivalic acid was poured through a paper filter to the preliminarily filtered hot solution of $Fe_2NiO(Piv)_6(HPiv)_3$. The onset of precipitation was observed in 5–100 min. After 24 h, the precipitate was filtered off on a glass filter, washed with hot DMF (10 mL) and acetonitrile (20 mL), and dried in air. The yield was ~60–75%. For sorption measurements, the obtained samples were dried in vacuo at 155°C.

Analyses for the samples dried in vacuo are the following.

$[Fe_2NiO(Piv)_6(L^1) \cdot 0.8HPiv \cdot 0.75H_2O]_n$ ($\mathbf{I}^D \cdot 0.8HPiv \cdot 0.75H_2O$; $x = 1.00$).

For $C_{54}H_{77.5}N_4O_{15.35}Fe_2Ni$			
anal. calcd., %:	C, 54.11;	H, 6.51;	N, 4.67.
Found, %:	C, 54.03;	H, 6.41;	N, 4.58.

$[Fe_2CoO(Piv)_6(L^1) \cdot 0.65H_2O]_n$ ($\mathbf{II}^D \cdot 0.65H_2O$; $x = 1.00$).

For $C_{50}H_{69.3}N_4O_{13.65}Fe_2Co$			
anal. calcd., %:	C, 53.84;	H, 6.26;	N, 5.02.
Found, %:	C, 53.80;	H, 6.26;	N, 5.00.

$[Fe_2NiO(Piv)_6(L^2) \cdot 0.5CH_3CN \cdot 0.45H_2O]_n$ ($\mathbf{III}^D \cdot 0.5CH_3CN \cdot 0.45H_2O$; $x = 1.00$).

For $C_{49}H_{68.4}N_{6.5}O_{13.45}Fe_2Ni$			
anal. calcd., %:	C, 51.91;	H, 6.08;	N, 8.03.
Found, %:	C, 51.90;	H, 6.09;	N, 8.01.

$[Fe_2CoO(Piv)_6(L^2) \cdot 0.7CH_3CN \cdot 0.25H_2O]_n$ ($\mathbf{IV}^D \cdot 0.7CH_3CN \cdot 0.25H_2O$; $x = 1.00$).

For $C_{49.4}H_{68.6}N_{6.7}O_{13.25}Fe_2Co$			
anal. calcd., %:	C, 52.11;	H, 6.07;	N, 8.24.
Found, %:	C, 52.38;	H, 6.01;	N, 8.30.

Synthesis of single crystals of $[Fe_2MO(Piv)_6(L^1)]_n$. $Fe_2NiO(Piv)_6(HPiv)_3$ (15 mg, 13.6 μmol) was dissolved in chloroform (10 mL), and the obtained solution was placed in a tube. Dioxane (5 mL) and a solution (10 mL) containing ligand L^1 (7 mg, 22.6 μmol) in ethanol (10 mL) were consecutively layered above the solution in the tube. Several weeks after, hexagonal single crystals that formed were collected for X-ray diffraction analysis.

Elemental analyses to C, H, and N were carried out on a Carlo Erba C, H, N analyzer. The microstructures of the samples were studied by SEM on the Carl Zeiss NVision 40 working station at accelerating voltages of 1–30 kV using a detector of secondary and secondary-scattered electrons. The detection was carried out without the preliminary sputtering of conducting materials on the sample surface. Electron probe X-ray microanalysis was carried out using an Oxford Instruments X-Max detector. The adsorption isotherms of N_2 and H_2 were determined using a Sorptomatic 1990 instrument at 78 K. X-ray phase analysis was carried out with a Bruker D8 ADVANCE diffractometer (CuK_α radiation, $\lambda = 1.54056$ Å).

The X-ray diffraction analysis of a single crystal of complex **I** was carried out on a Bruker Apex II diffractometer (CCD detector, MoK_α, $\lambda = 0.71073$ Å, graphite monochromator) [11]. The structure was solved by direct methods and refined in the full-matrix anisotropic approximation for all non-hydrogen atoms. The hydrogen atoms at the carbon atoms of the organic ligands were geometrically generated and refined in the riding model. The calculations were performed using the SHELX-97 program package [12]. The disordered solvate molecules in compound **I** that were not localized were removed using the SQUEEZE procedure [13]. The crystallographic parameters and details for structure refinement are the following: brown orthorhombic crystals, $0.10 \times 0.10 \times 0.10$ mm in size, $C_{51}H_{69}N_3O_{13}Fe_2Ni$, 1102.62 g/mol, $T =$ 150(2) K, trigonal crystal system, space group $P\bar{3}1c$, $a = 16.83(4)$, $c = 15.27(3)$ Å, $V = 3745(1)$ Å^3, $Z = 4$, $\rho_{calcd} = 0.987$ g/cm^3, $\mu = 0.676$ mm^{-1}, $\theta_{max} = 25.69°$, number of measured reflections 31793, number of independent reflections 2394, $R_{int} = 0.437$, goodness-of-fit 0.766, R_1 ($I > 2\sigma(I)$) = 0.1143, wR_2 ($I > 2\sigma(I)$) = 0.2622. The coordinates of atoms and other parameters for structure **I** were deposited with the Cambridge Crystallographic Data Centre (CCDC 1035537; deposit@ccdc.cam.ac.uk or http://www.ccdc.cam.ac.uk/data_request/cif).

RESULTS AND DISCUSSION

The reactions of trinuclear pivalates $Fe_2MO(Piv)_6(HPiv)_3$ (M = Co and Ni) with L^1 or L^2 in different solvents (DMF and chloroform) lead to formation compounds of the composition $[Fe_2MO(Piv)_6(L)]_n$. The composition of the samples synthesized in chloroform differs from the stoichiometric one (the composition of the samples is given in Experimental, and possible reasons for the deviation of the composition from the stoichiometric one are discussed below). The samples of $[Fe_2MO(Piv)_6(L)]_n$ ($L = L^1$ and L^2) crystallize from chloroform and DMF and have similar structures, which is indicated by their powder diffraction patterns (the typical diffraction patterns are presented in Fig. 1).

According to the SEM data, the samples obtained from DMF consist of regular hexagonal crystals with an average size of ~20 μm and a thickness of ~3 μm (Fig. 2). The samples obtained from chloroform consist of irregular crystals ~1–2 μm in size. The XPRD data are consistent with the SEM data. According to the XPRD data, the reflection broadening in the powder diffraction patterns of the freshly prepared (from DMF) samples corresponds to the instrumental broadening within the error, indicating the high crystallinity and a large size of the crystallites. On the contrary, the samples obtained from chloroform are characterized by broader reflections, which can be due to a

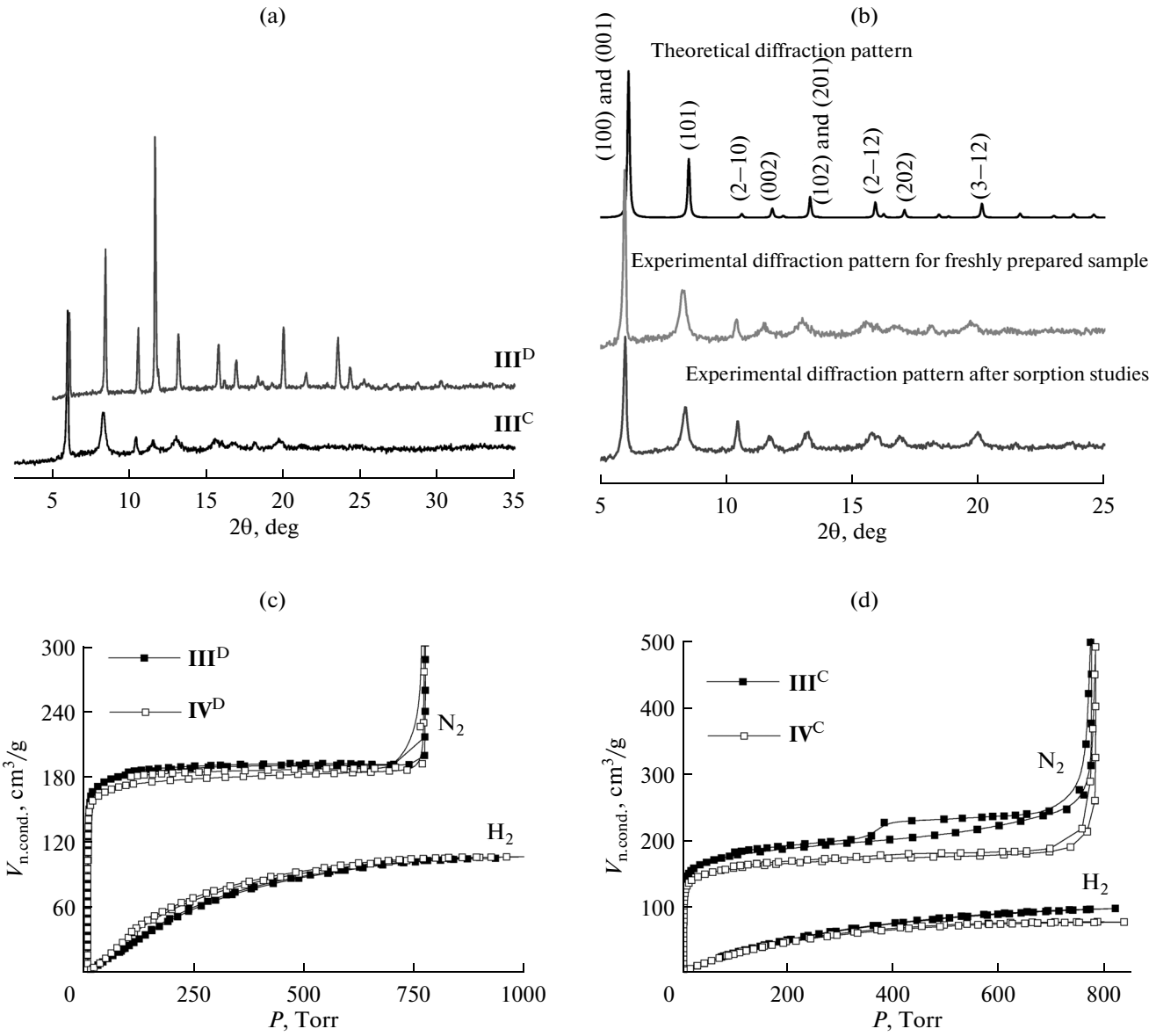

Fig. 1. Diffraction patterns of samples (a) $\mathbf{III}^{D}$ and $\mathbf{III}^{C}$ and (b) $\mathbf{IV}^{C}$ before and after the thermal treatment ($\lambda = 1.54056$ Å); the nitrogen and hydrogen adsorption isotherms ($T = 78$ K) by samples (c) $\mathbf{III}^{D}$ and $\mathbf{IV}^{D}$ and (d) $\mathbf{III}^{C}$ and $\mathbf{IV}^{C}$. The volumes of nitrogen and hydrogen sorbed by the samples were reduced to normal conditions (n.cond.): 273.15 K, 101.3 kPa.

smaller size of the crystallites or a higher content of defects in them.

The exterior of crystals of compounds $[Fe_2MO(Piv)_6(L)]_n$ (L = L^1 and L^2) remains almost unchanged on heating in vacuo necessary for the removal of the solvent from these compounds prior to sorption studies. The powder diffraction patterns of these complexes somewhat differ after the thermal treatment, but the position of all reflections remains unchanged (Fig. 1b).

Single crystals of compound **I** obtained by the slow diffusion of the reagents in a $CHCl_3$–C_2H_5OH–dioxane (2 : 2 : 1 vol/vol/vol) mixture are isostructural to the crystals of the previously described compound **I** · 3DMSO · $0.84H_2O$ [8] (DMSO is dimethyl sulfoxide; the unit cell parameters for compounds **I** and **I** · 3DMSO · $0.84H_2O_3$ are 16.667(5) and 16.775(2) Å for *a*, 14.966(4) and 14.973(1) Å for *c* (at 150 K), respectively). Since structure **I** · 3DMSO · $0.84H_2O$ was published [8], only the main characteristics of crystal structure **I** are presented in this work. Compound **I** is built of parallel 2D polymer layers according to the honeycomb type. Three pyridine fragments of three L^1 molecules are coordinated to the trigonal fragments $\{Fe_2NiO(Piv)_6\}$ at an angle of 120° in each 2D layer (Fig. 3). In turn, each ligand L^1 binds three metal ions of three fragments $\{Fe_2NiO(Piv)_6$ at the same angle. Thus, the topology of 2D layers in structure **I** is deter-

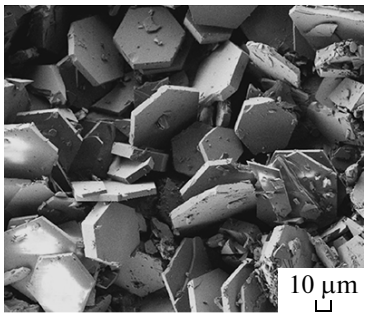

$[Fe_2NiO(Piv)_6(L^1)]_n$ (**I**^{D}) from DMF

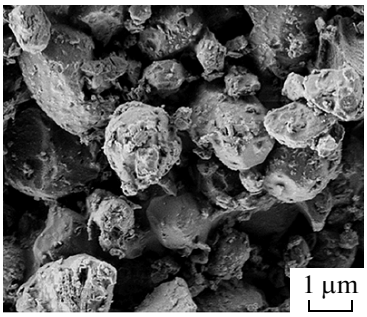

$[Fe_2NiO(Piv)_6(L^1) \cdot 0.43Fe_2NiO(Piv)_6]_n$ (**I**^{C}) from $CHCl_3$

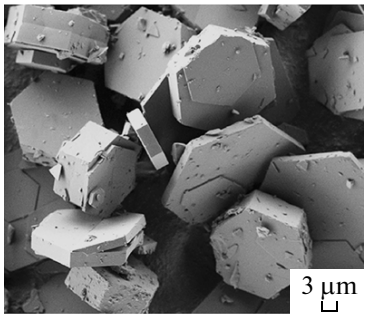

$[Fe_2CoO(Piv)_6(L^1)]_n$ (**II**^{D}) from DMF

$[Fe_2CoO(Piv)_6(L^1) \cdot 0.18Fe_2CoO(Piv)_6]_n$ (**II**^{C}) from $CHCl_3$

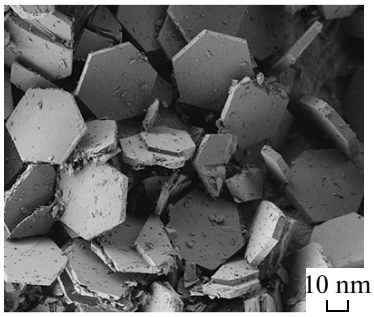

$[Fe_2NiO(Piv)_6(L^2)]_n$ (**III**^{D}) from DMF

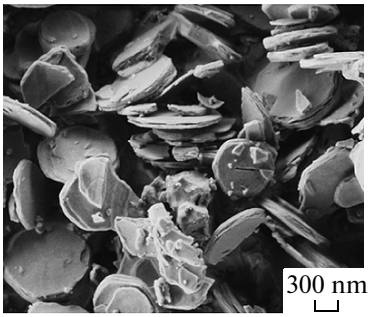

$[Fe_2NiO(Piv)_6(L^2) \cdot 0.075L^2]_n$ (**III**^{C}) from $CHCl_3$

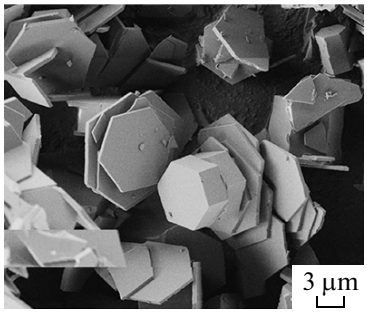

$[Fe_2NiO(Piv)_6(L^2)]_n$ (**IV**^{D}) from DMF

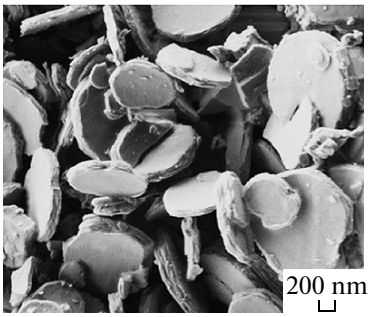

$[Fe_2CoO(Piv)_6(L^2) \cdot 0.17L^2]_n$ (**IV**^{C}) from $CHCl_3$

Fig. 2. SEM images of the studied samples.

mined by the symmetry of components of the building fragments. The mutual orientation of the parallel 2D layers is shown in Fig. 4. As in the case of compound **I** · 3DMSO · 0.84H_2O [8], channels are formed along the z axis of the crystal lattice of compound **I**. The channels can be presented as cavities (diameter ~10.6 Å = 7.8 + 2r; the value was obtained using the Mercury software for a probe molecule with the radius

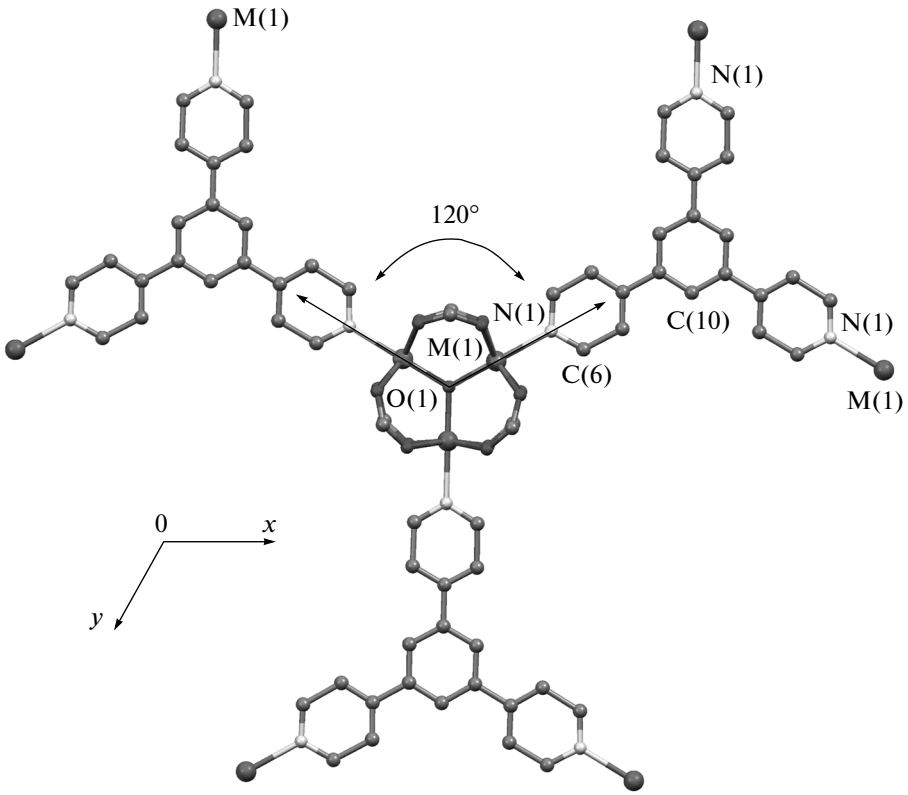

Fig. 3. Fragment of the crystal lattice of compound **I** (M = Fe and Ni with filling factors of 2/3 and 1/3, respectively). *tert*-Butyl groups and all hydrogen atoms are omitted. The N atoms of the central pyridine molecule cannot be localized by X-ray diffraction analysis because of the C_3 axis passing through the central ring (for this reason, all atoms were determined as carbon atoms). The metal ions of the adjacent units are additionally shown. The solvent molecules are not localized.

r = 1.4 Å "touching" the cavity walls) separated by "windows" (diameter ~6.4 Å = 3.6 + 2r). The theoretical diffraction pattern of compound **I** coincides with those obtained experimentally for samples $\mathbf{I}^{D}$ and $\mathbf{I}^{C}$ from DMF or chloroform, respectively. Thus, a change of the synthesis conditions (reaction temperature and solvent) does not change the crystallographic parameters, unlike the porous coordination polymers with coordinatively labile crystal lattice [14] or those built of 1D chains [15].

The character of peak broadening for the samples obtained from chloroform can be related to both a small size of the crystallites and the existence of microstrains. The contributions of these factors can be distinguished by the dependence of the reflection broadening β (determined as a reflection width at the half-height) on the diffraction angle. If the broadening is caused by a small crystallite size, the reflection width depends on the angle as $\beta = \lambda/(L\cos(\theta))$ (L is the crystallite size, and λ is the wavelength) and is inversely proportional to cos(θ). If the broadening is due to microstrains in the crystallites, then $\beta = 2\tan(\theta)\,\Delta a/a$ (θ is the diffraction angle, a is the interplanar distance, and Δa is the deviation of the interplanar distance from the average value), and the reflection width is proportional to tan(θ) in this case [16]. A conclusion about the reason for the reflection broadening can be made by comparing β_1/β_2 with $\cos(\theta_2)/\cos(\theta_1)$ or $\tan(\theta_1)/\tan(\theta_2)$, where the indices refer to reflections with multiple *hkl* (the fulfillment of the criterion of *hkl* multiplicity of compared reflections is important, because the planes with different *hkl* can be arranged in different directions in which the linear sizes of the crystal differ substantially). The values of β_1/β_2 with $\cos(\theta_2)/\cos(\theta_1)$ were compared or $\tan(\theta_1)/\tan(\theta_2)$ for the reflections with *hkl* {101} and {202}. For the samples freshly prepared from chloroform, β_1/β_2 is equal to $\tan(\theta_1)/\tan(\theta_2)$ within the error of measuring the reflection half-width and exceeds the $\cos(\theta_2)/\cos(\theta_1)$ ratio, which can be due to the nonideal character of the crystal lattice (in particular, due to many dislocations, displacements of individual 2D layers, etc.). After activation and sorption measurements, β_1/β_2 decreases but remains close to $\tan(\theta_1)/\tan(\theta_2)$ within the measurement error. Thus, the reflection broadening in the diffraction patterns of the samples synthesized in chloroform is due to strains in the crystals rather than the small size.

The differences in sizes, crystal shapes, and ordering (crystallinity) of the $[Fe_2MO(Piv)_6(L)]_n$ (L = L^1

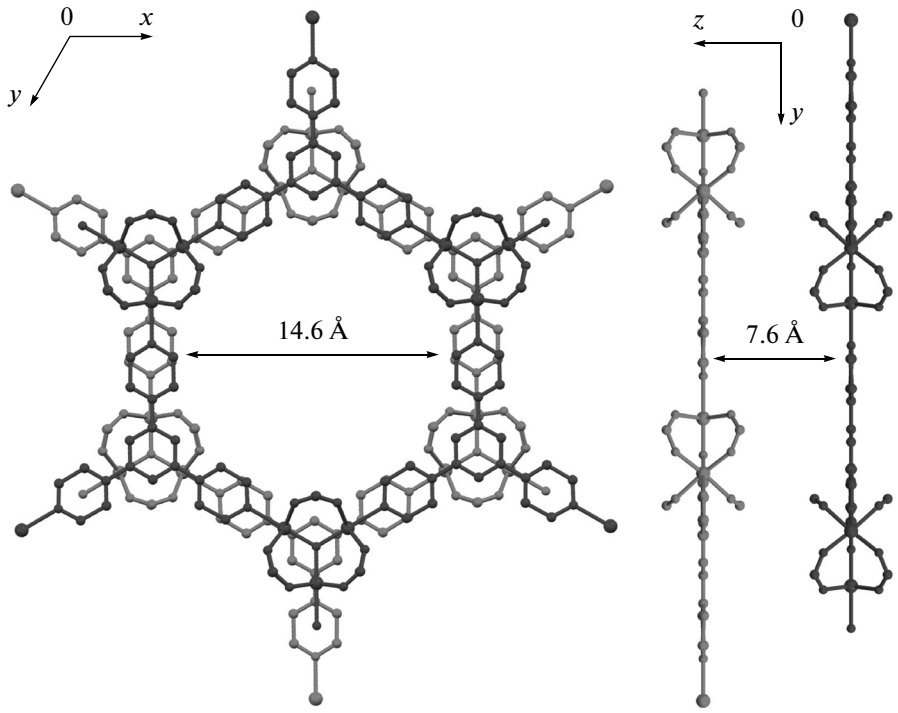

Fig. 4. Fragments of two adjacent 2D layers of compound **I**. *tert*-Butyl groups and all hydrogen atoms are omitted, and the solvent molecules are not localized. Distances of 7.6 Å correspond to the distance between the planes passed through the centers of the metal ions and μ_3-O of two adjacent 2D layers.

and L^2) samples obtained from different solvents can be explained by different crystallization rates. In turn, the crystallization rate affects the closeness of crystallization to the idealized equilibrium state. All starting substances (both the trinuclear complexes $Fe_2MO(Piv)_6(HPiv)_3$ and ligands) are soluble in both DMF and chloroform. Probably, the intermediate reaction products (for example, discrete compounds $Fe_2MO(Piv)_6(L)_n$ or $\{Fe_2MO(Piv)_6\}_n(L)$ (n = 1–3), which are formed upon the formation of a coordination polymer) are better soluble in DMF than in chloroform. The reaction of the trinuclear complexes $Fe_2MO(Piv)_6(HPiv)_3$ with the tripyridine ligands in chloroform rather rapidly affords poorly soluble products, being crystallization sites of new crystals. This assumption is favored by noticeable deviations of the composition of the complexes $[Fe_2MO(Piv)_6(L)]_n$ (L = L^1 and L^2) from the stoichiometric one (the ratio of the content of the trinuclear moiety to that of the ligand is 1 : 1). For example, compounds $Fe_2NiO(Piv)_6(L^1) \cdot 0.43Fe_2NiO(Piv)_6$ (**I**^{C}) or $Fe_2CoO(Piv)_6(L^1) \cdot 0.18Fe_2CoO(Piv)_6$ (**II**^{C}) are formed in chloroform, whereas coordination polymers with the composition very close to the stoichiometric composition 1 : 1 are formed in DMF. The dependence of the growth rate of the crystal lattice in different crystallographic directions on the solvent cannot be excluded.

The shape of the nitrogen adsorption isotherms for all the compounds is typical of microporous sorbents (isotherms of type I according to the IUPAC classification [17]). A sharp increase in the isotherms at low pressures corresponds to micropore filling, after which the sorption capacity does not nearly increase below p/p_S about 0.95. An increase in the isotherms at the pressure approaching p_S can be explained by the interparticle condensation of nitrogen. The nitrogen adsorption isotherms of all complexes, except **III**^{C}, contain no hysteresis of adsorption and desorption, whereas a small deviation between the nitrogen adsorption and desorption curves is observed in the case of **III**^{C}.

The surface areas of the complexes were calculated from the nitrogen adsorption isotherms using the BET equation, and the values of pore volume were calculated by commonly accepted methods using the Dubinin–Radushkevich equation [17]. A comparison of the sorption characteristics of the samples (table) obtained from DMF and chloroform shows that an increase in the crystallinity (determined from the combined data of X-ray phase analysis and SEM as described above) and crystal size decreases the specific surface area by 50–100 m^2/g, and the micropore volume decreases by 0.02–0.04 cm^3/g (7–14% in both cases). The sorption capacity with respect to hydrogen decreases by 0.18 wt % on going from samples **I**^{D} and **IV**^{D} to samples **I**^{C} and **IV**^{C} (by approximately 1.25 times), whereas the decrease in the capacity is 0.08 wt % (by approximately 1.1 times) for a series of

Sorption characteristics of compounds $Fe_2MO(Piv)_6(L^1)$ and $Fe_2MO(Piv)_6(L^2)$ (M = Co and Ni)

Compound*	S_{BET}, m^2/g	$V_{micropore}$, cm^3/g**	$u(H_2)$, %***
$[Fe_2NiO(Piv)_6(L^1)]_n$ ($\mathbf{I}^D$)****	730	0.28	0.91
$[Fe_2NiO(Piv)_6(L^1) \cdot 0.43Fe_2NiO(Piv)_6]_n$ ($\mathbf{I}^C$)	630	0.26	0.73
$[Fe_2CoO(Piv)_6(L^1) \cdot 0.18Fe_2CoO(Piv)_6]_n$ ($\mathbf{II}^C$)	610	0.26	0.77
$[Fe_2NiO(Piv)_6(L^2)]_n$ ($\mathbf{III}^D$)	730	0.29	0.93
$[Fe_2NiO(Piv)_6(L^2) \cdot 0.075L^2]_n$ ($\mathbf{III}^C$)	680	0.27	0.85
$[Fe_2CoO(Piv)_6(L^2)]_n$ ($\mathbf{IV}^D$)	690	0.28	0.85
$[Fe_2CoO(Piv)_6(L^2) \cdot 0.17L^2]_n$ ($\mathbf{IV}^C$)	610	0.24	0.67

* The solvent used for the crystallization of the complexes is DMF for $\mathbf{I}^D$–$\mathbf{IV}^D$ and $CHCl_3$ for $\mathbf{I}^C$–$\mathbf{IV}^C$.

** Calculated by the Dubinin–Radushkevich model.

*** The maximum attained experimental value.

**** Data from [8].

samples $\mathbf{III}^D$ and $\mathbf{III}^C$. A decrease in the sorption characteristics with a decrease in the crystallinity can be due to both blocking some pores because of crystal defects and the possible presence of nonporous intermediate reaction products as an individual phase.

The sorption capacity with respect to hydrogen for the samples studied in this work correlates with both the surface area and pore volume of the sorbents. The corresponding dependences can be approximated by linear Eqs. (1) and (2), respectively.

$$u(H_2, \%) = aS_{BET} + \text{const}, \quad (1)$$

$$u(H_2, \%) = bV_{DR} + \text{const}. \quad (2)$$

In these equations, u designates the hydrogen uptake (%), a is the weight of hydrogen (g) sorbed on 1 m^2 of the surface (×100), and b is the density of hydrogen in micropores (g/cm^3) ×100).

The value of $a = 8.0(1) \times 10^{-4}$ g/m^2 (const = 0.06) determined in terms of this approach for the porous coordination polymers described in this work is approximately 30% of the theoretically possible limit of the monolayer filling (accepting that 1 molecule occupies 0.14 nm^2 [18], the maximum possible value of a is at a level of 2.37×10^{-3} g/m^2). The determined value of $b = 1.1(1)$ g/cm^3 (const = 0.11) corresponds to the hydrogen density $d(H_2) = 0.01$ g/cm^3, which is lower than the density of liquid hydrogen at the boiling point (0.071 g/cm^3 at 20.3 K and 1 atm) or at the critical point (0.031 g/cm^3 at 33 K and 12.8 atm).

There are many *tert*-butyl groups in the pore walls of the complexes described in this work. In the case of the porous coordination polymers, whose pore walls are predominantly built of aromatic rings [19], the value of parameter a is approximately 2.5 times higher than that for the compounds described in this work and is equal to $2.1(1) \times 10^{-3}$ g/m^2, which is almost 90% of the theoretical limit of the monolayer filling. The value of b is tenfold lower than that for the porous coordination polymers and is equal to 0.1 g/cm^3 [19]. In the case of the carbon sorbents, the value of a ranges from 4.2×10^{-4} to 1.2×10^{-3} g/m^2, depending on the sorbent structure, whereas coefficient b is 1.06–4.6 g/cm^3 [18, 20, 21]. For porous SiO_2 and Al_2O_3 [18] and composites MSM-41 with nanoparticles of 3*d* metals or their oxides [22], the values of parameters a (7.6×10^{-4} and 4.7×10^{-4} g/m^2) and b (4.4 g/cm^3) also fall onto these ranges. Thus, in the case of the porous coordination polymers, whose walls are mainly formed by *tert*-butyl groups and whose structure includes aromatic fragments of ligands of the bi- and tripyridine series, the sorption capacity with respect to hydrogen is mainly determined by micropores rather than by the surface area. The contribution of micropores in the porous coordination polymers considered in this work is comparable with the micropore contribution to the sorption capacity with respect to hydrogen of some classes of carbon sorbents. At the same time, the influence of the surface area is higher than the micropore effect for the porous coordination polymers in which the pore walls are formed by aromatic groups and in which hydrogen can be bound near metal ions [19, 23–25]. This can be due to a higher polarizing effect of aromatic groups on hydrogen molecules and, as a consequence, to a denser monolayer filling. For the porous sorbents in which the pores are formed by oxygen ions (porous SiO_2 and Al_2O_3 and composites MSM-41 with 3*d*-metal nanoparticles), the influence of the pore volume is stronger than that for the compounds described in this work.

Thus, the study of the sorption characteristics of the samples of porous coordination polymers $[Fe_2MO(Piv)_6(L)]$ (where M = Co and Ni, L is tris(4-pyridyl)pyridine (L^1) or tris(4-pyridyl)triazine (L^2)) consisting of crystals of different average sizes (from 1 to 20 μm) shows that an increase in the average crystal size and the enhancement of the crystallinity lead to an increase in the sorption capacity with respect to hydrogen from 0.7 to 0.9% (78 K, 1 atm). According to the criteria of efficiency of hydrogen filling of the surface and micropores, the porous coordination polymers described in this work occupy an intermediate

place between the porous coordination polymers, whose pore walls are predominantly formed by aromatic rings, and the porous sorbents based on SiO_2 or Al_2O_3.

ACKNOWLEDGMENTS

This work was supported by the target complex program for research of the National Academy of Sciences of Ukraine "Hydrogen in Alternative Power Engineering and New Technologies," the Russian Academy of Sciences, and the Council on Grants at the President of the Russian Federation (grant no. NSh-4773.2014.3).

REFERENCES

1. Foo, M.L., Matsuda, R., and Kitagawa, S., *Chem. Mater.*, 2014, vol. 26, p. 310.
2. Kitagawa, S., Kitaura, R., and Noro, S., *Angew. Chem.*, 2004, vol. 116, p. 2388.
3. Rowsell, J.L.C., Millward, A.R., Park, K.S., and Yaghi, O.M., *J. Am. Chem. Soc.*, 2004, vol. 126, p. 5666.
4. Burrows, A.D., *CrystEngComm*, 2011, vol. 13, p. 3623.
5. Tanaka, D., Henke, A., Albrecht, K., et al., *Nat. Chem.*, 2010, vol. 2, p. 410.
6. Dorofeeva, V.N., Kolotilov, S.V., Kiskin, M.A., et al., *Chem.-Eur. J.*, 2012, vol. 18, p. 5006.
7. Polunin, R.A., Kolotilov, S.V., Kiskin, M.A., et al., *Eur. J. Inorg. Chem.*, 2010, p. 5055.
8. Polunin, R.A., Kiskin, M.A., Cador, O., and Kolotilov, S.V., *Inorg. Chim. Acta*, 2012, vol. 380, p. 201.
9. Smith, C.B., Raston, C.L., and Sobolev, A.N., *Green Chem.*, 2005, vol. 7, p. 650.
10. Barrios, L.A., Ribas, J., and Aromi, G., *Inorg. Chem.*, 2007, vol. 46, p. 7154.
11. *SMART (Control) and SAINT (Integration) Software. Version 5.0*, Madison (WI, USA): Bruker AXS Inc., 1997.
12. Sheldrick, G.M., *Acta Crystallogr., Sect. A: Found. Crystallogr.*, 2008, vol. 64, p. 112.
13. Spek, A.L., *Acta Crystallogr. Sect. D: Biol. Crystallogr.*, 2009, vol. 65, p. 148.
14. Polunin, R.A., Kolotilov, S.V., Kiskin, M.A., et al., *Eur. J. Inorg. Chem.*, 2011, p. 4985.
15. Polunin, R.A., Burkovskaya, N.P., Kolotilov, S.V., et al. *Russ. Chem. Bull. Int. Ed.*, 2014, vol. 63, p. 252.
16. Kovba, L.M. and Trunov, V.K., *Rentgenofazovyi analiz* (Powder X-ray Diffraction), Moscow: MGU, 1976.
17. Gregg, S.J. and Sing, K.S.W., *Adsorption, Surface Area, and Porosity*, New York: Academic, 1991.
18. Nijkamp, M.G., Raaymakers, J.E.M.J., van Dillen, A.J., and de Jong, K.P., *Appl. Phys. A*, 2001, vol. 72, p. 619.
19. Kolotilov, S.V. and Pavlishchuk, V.V, *Theor. Exp. Chem.*, 2009, vol. 45, p. 75.
20. Vasiliev, L.L., Kanonchik, L.E., Kulakov, A.G., et al., *Int. J. Hydrogen Energy,* 2007, vol. 32, p. 5015.
21. Pang, J., Hampsey, J.E., Wu, Z., et al., *Appl. Phys. Lett.*, 2004, vol. 85, p. 4887.
22. Kolotilov, S.V., Shvets, A.V., and Kas'yan, N.V., *Theor. Exp. Chem.*, 2006, vol. 42, no. 5, p. 271.
23. Spencer, E.C., Howard, J.A.K., McIntyre, G.J., et al., *Chem. Commun.*, 2006, p. 278.
24. Yildirim, T. and Hartman, M.R., *Phys. Rev. Lett.*, 2005, vol. 95, p. 215504.
25. Kolotilov, S.V. and Pavlishchuk, V.V., *Theor. Exp. Chem.*, 2009, vol. 45, no. 5, p. 277.

Translated by E. Yablonskaya